Research Article

Synthesis of silver nanoparticle from *Vigna unguiculata* stem as adsorbent for malachite green in a batch system

Folasegun A. Dawodu[1] · Courage U. Onuh[1] · Kovo G. Akpomie[2] · Emmanuel I. Unuabonah[3]

Abstract

This study describes a simple and cost effective method for the synthesis of silver nanoparticles from locally available *Vigna unguiculata L.* stem extract, as alternative method to the expensive and toxic chemicals used, and its application as adsorbent for malachite green (MG) in a Batch system. The AgNPs were synthesized using $AgNO_3$ as precursor and stem extract as reducing and capping agent. The AgNPs were characterized using UV–Vis, SEM-EDX, FTIR and XRD. The effects of contact time, pH of solution, initial dye concentration, adsorbent concentration and temperature were studied and they proved useful in the description of the adsorption process. AgNPs showed SPR bands at 455 nm. The XRD micrographs showed face centered cubic crystal structure with average crystalline size of the synthesized nanoparticle of ~ 25 nm. Alkaloids present in *Vigna unguiculata L.* stem played a role in the reduction of $AgNO_3$. An optimum pH of adsorption was achieved at 9.0. The adsorption process was observed to be exothermic. Equilibrium isotherm models showed Langmuir isotherm with R^2 of 0.99194 and residual sum of squares (RSS) of 5.23541×10^{-5}, indicating monolayer adsorption. Kinetic studies revealed Pseudo-first order kinetics best fitted the rate of adsorption and intra-particle diffusion revealed that the adsorption process was controlled by surface phenomenon and intra-particle diffusion. The results showed the applicability of AgNPs in adsorption. However, the relatively low percentage removal (21.6% at 200 ppm) suggests that Silver nanoparticle synthesized from *Vigna unguiculata L.* stem, alone may not be sufficient in the complete adsorption of MG dye.

Keywords Biosynthesized AgNPs · Adsorption · MG · Adsorption isotherm · Kinetics

1 Introduction

The discharge of dye-containing wastewater in various industries, like food, printing, textiles, dyeing and dye stuff manufacturing industries, has become of great environmental concern due to toxicological and aesthetical reasons. Dye wastewaters occur mostly as a result of the inefficiencies in the dyeing process during which a sizeable amount of the used dye enters the aquatic environment as wastes resulting in colored effluents [1]. Dye wastewaters are toxic and have been known to cause a serious hazard on health, aquatic organisms and affect human activities. Most of the dyes discharged from industries are synthetic, containing complex aromatic rings of large molecular size which makes them stable against photo-bleaching, resistant to biologically degradation and aerobic digestion [2].

Whilst numerous technologies including membrane filtration, reverse osmosis, and electrochemical methods have been applied worldwide to remove dyes from water, the development of an economic, effective and rapid water treatment at a large scale remains a challenging issue. Adsorption technology is considered to be the most auspicious and robust method to purify aqueous solutions at low cost and with high-efficiency [1, 2]. This technique

✉ Kovo G. Akpomie, kovo.akpomie@unn.edu.ng | [1]Department of Chemistry (Industrial), University of Ibadan, Ibadan, Nigeria. [2]Department of Pure & Industrial Chemistry, University of Nigeria, Nsukka, Nigeria. [3]Department of Chemical Sciences, Redeemers's University, Redemption City, Mowe, Nigeria.

SN Applied Sciences (2019) 1:346 | https://doi.org/10.1007/s42452-019-0353-3

Received: 9 January 2019 / Accepted: 7 March 2019 / Published online: 15 March 2019

has been found to be beneficial above other techniques in terms of initial cost, ease of implementation, insensitivity to toxic substances, simplicity of design and capability to remove dyes at low concentrations as opposed to other techniques where purification becomes less effective at very low contaminant concentration.

All adsorption process comprises of the transfer of undesirable chemicals, in this case dye, from a liquid or gas to the surface of a solid adsorbent in a transient process. The ability of adsorption process to remove pollutants is solely limited by the capacity of the adsorbent itself. Once saturated, pollutants can no longer be removed from a solution. Clay based adsorbents [2], sawdust [3], nanoparticles, and other low cost adsorbents have been employed to remove MG from water. Nanoparticle adsorption however is an emerging technique in the area of removal of dyes. Large scale adsorption with any suitable adsorbent can be carried out either in batch mode or a fixed bed adsorption mode. Batch adsorption process are less expensive and best suited for small scale operations where the adsorption step is not continuously demanded and a long contact time is required [4].

Vigna unguiculata L. Walp. is one of the most widely adaptable, and salubrious grain legumes grown in moderately hot to hot regions of Africa, Asia, and the Americas. It is a dicotyledonous plant of the family of Papilionaceae (Leguminosae- Papilionoideae, Fabaceae), belonging to the sub-family, Fabiodeae [5].

Africa accounts for about 75% [6], whilst Nigeria is the largest producer and consumer, accounting for about 45 percent of its world's production [7]. Its common names include: Cowpea (English), beans (Nigeria), ewa (Yoruba), Wake (Hausa) and Agwa (Igbo). Islam et al. [8] emphasized that all parts of the plant used as food are nutritious providing protein and vitamins. It is chiefly a vegetable and grain crop for human. Cowpea is valued as a nutritional supplement to cereals and an extender of animal proteins, and it serves as a very safe fodder for livestock animals [9]. Cowpea has high level of folic acid and low levels of antinutritional and flatulence producing factors [10]. However, after harvesting of the cowpea, the stems are of little significant value and are mainly utilized for burning purposes.

Malachite green (MG) is a well-known dye used for dyeing of leather, wool, silk, used as fungicide, ecto-parasiticide in aquaculture and fisheries due to the low cost, availability, efficacy and lack of a proper alternative [11]. MG is a water soluble cationic dye that belongs to triphenylmethane category, containing two amino groups. It dissociates into anion and coloured cations. MG dyes are mutagenic and carcinogenic in nature and is severely toxic to a wide range of aquatic life. Conventional water treatment techniques have been found to be inefficient in the treatment of MG due to the low biodegradability of the dye.

There are few publications on the use of silver nanoparticle alone as adsorbent for MG and other dyes from water [12–16]. Although found to be efficient, none of the report has provided insight on the adsorptive removal of MG using silver nanoparticle (AgNPs) synthesized from *Vigna unguiculata L*. The readily available stem of *Vigna unguiculata L*. could possibly be utilized as low cost material for synthesis of AgNPs for MG removal. Hence, the objectives of the present study was to develop an alternative cost effective synthetic route for AgNPs using aqueous stem extract of *Vigna unguiculata* L. and to evaluate the performance as adsorbent for MG using batch adsorption method.

2 Materials and methods

2.1 *Vigna unguiculata* stem processing

Fresh stem samples were obtained from farms in New Nyanya, Nasarawa, Nigeria. The stems were cleaned with running tap water and then with distilled water. The stems were cut into smaller pieces for extraction and air dried at room temperature. The sample was pulverized and used for extraction with distilled water.

2.2 Moisture content

Three grams of fresh stem was weighed into a preweighed crucible and heated at 105 °C for 4 h to constant weight. After which the sample in the crucible was cooled in the desiccator and then weighed. The Moisture content was calculated by the difference in wet and dry weight:

$$\text{Moisture Content}\,(\%) = \frac{\text{Wet weight} - \text{Dry weight}}{\text{Wet weight}} \times 100\% \quad (1)$$

2.3 Preparation of the *Vigna unguiculata* stem extract

Forty grams of finely cut/pulverized stem was kept in a beaker containing 400 mL distilled water and boiled for 45 min. The extract was cooled down and filtered with Whatman filter paper no.1. The filtrates were stored at 4 °C for silver nanoparticle synthesis.

2.4 Green synthesis and characterization of silver nanoparticles

The plant extract (50 mL) was added to 100 mL of 0.01 M concentrations of aqueous silver nitrate solution. The resulting mixture was allowed to stand for 5 h. The bioreduction of Ag^+ ions to Ag^0 was monitored by taking

samples at 1 h intervals of reaction time using UV–Vis spectrophotometer. Its formation was also confirmed by using UV–Visible spectroscopy (UV–Vis Double Beam 8 Auto cell UVS 2700 Spectrophotometer). The resulting AgNPs pellet (which sedimented after some time) was collected, washed and dried at 80 °C in an oven.

Fourier transform infrared spectroscopy (FTIR) studies were carried out for both unloaded and MG-loaded AgNPs using Perkin Elmer FTIR Spectrum BX having a resolution of 32 cm^{-1} in wavelength region 350–4400 cm^{-1} in KBr pellets. It was used to identify the presence of biomolecules and functional group which may support the capping and stabilization by the stem extract.

The surface morphology of the synthesized AgNPs was determined from SEM (JOEL JSM 7600F). The crystallinity and crystal phases of the AgNPs was characterized by X-ray diffraction (XRD, Rigaku D/Max-IIIC) pattern measured with Cu-Kα Radiation (λ = 1.556 Å) in the range of 20–80.

The point of zero charge of the synthesized AgNPs was determined by Salt addition method. In this method, a weighed amount (0.05 g) of AgNPs was added to 10 mL of 0.01 M NaCl solution in 100 mL conical flask with pH ranging from 2–12. The initial pH of the solution was adjusted using 0.1 M NaOH or HCl. AgNPs (0.05 g) adsorbent was added to each flask. The conical flasks were shaken for 24 h after which the final pH values were measured. The difference between the initial and final pH was calculated and plotted against the initial pH. The pH_{pzc} was obtained from the point of intersection with pH axis.

2.5 Adsorbate characteristics and preparation

Malachite green dye is widely used in textile, paper and carpet industries. It is a basic cationic dye. Malachite green dye C.I. = 42,000B, CAS No. 2437-29-8, chemical formula = $C_{23}H_{26}N_{2O}$; λ_{max} = 611 nm (experimentally obtained) was manufactured by Kem light Laboratories PVT, India. 0.5 g weighed quantity of the dye was dissolved in 1000 mL deionized water to prepare stock solution. Experimental solutions of the desired concentration were obtained by dilution of stock solution.

2.6 Batch adsorption experiment

Effects of initial solution pH (3–12), contact time (5–60 min), AgNPs adsorbent concentration (0.4–2.0 g), initial MG dye concentration (50–300 mg/L) and temperature (30–50 °C) on the adsorption process were studied in batches. The pH of the adsorbate solution was adjusted with 0.1 M HCl or 0.1 M NaOH. AgNPs (1.0 g) was weighed and added to 20 mL of 200 mg/L MG solution in a 100-mL conical flask. The flasks were shaken in a thermo-stated shaker at 130 rpm for 30 min. The solution was centrifuged at 20,000 rpm for 10 min. Samples were taken from the flasks after a given time to analyze the concentration of malachite green in the solution. The residual amount of malachite green in each flask was investigated using UV–VIS spectrophotometer (SHIMADZU Brand UV-3000) at λ_{max} of 611.0 nm. The amount of dye adsorbed per unit AgNPs, q_e(mg dye/g adsorbent) was calculated according to a mass balance on the dye concentration using:

$$q_e = \frac{C_0 - C_e}{m} \times V \quad (2)$$

where C_0 and C_e (mg/L) are the dye concentrations at initial and at equilibrium, respectively. V is the volume of the solution (L) and m is the mass (g) of AgNPs adsorbent used.

2.7 Adsorption isotherms and kinetic modeling

The Adsorption isotherms were studied on the adsorption of MG dye on AgNPs using adsorption models like Langmuir, Freundlich, Tempkin and Dubinin–Radushkevich (D–R). The theory behind these isotherm equations have been discussed extensively [17]. The suitability of the isotherm equations to the equilibrium data obtained were compared by accessing the correlation coefficients, R^2 and residual sum of the squares (RSS). Linear regression was carried out by using OriginPro 2017 from OriginLab.

Adsorption kinetics studies provide vital information with regards to the time needed for reaching equilibrium, rate of adsorption process and adsorption potential rate limiting steps. The adsorption kinetics of adsorption of MG dye on AgNPs was investigated using pseudo-first order, pseudo-second-order, Elovich and intraparticle diffusion models. The equations and theory of the kinetic models have also been discussed extensively in literature [17].

2.8 Residual square of sums (rss)

Believed to be one of the most widely used error function was used to evaluate the best fit isotherm model. This error is represented as:

$$\chi 2 = \sum_{i=1}^{n} \left(q_{eCalc} - q_{eExp}\right)^2 \quad (3)$$

where q_{eCalc} (mg/g) is the theoretical concentration of MG dye on the AgNPs, calculated from one of the isotherm models. q_{eExp} (mg/g) is the experimentally measured adsorbed solid phase concentration of the MG dye adsorbed on AgNPs.

2.9 Nonlinear Chi–square test (χ^2)

This is one of the error analysis carried out to determination of the best fit of an adsorption system. The value of this function can be obtained from the equation:

$$\chi 2 = \sum_{i=1}^{n} \frac{\left(q_{eCalc} - q_{eExp}\right)^2}{q_{eExp}} \quad (4)$$

The best fit kinetic model was validated with non-linear Chi–square test (χ^2) and correlation coefficient (R^2). R^2 of the best fit model must be the closest to 1. Also, similarities between experimentally determined and calculated data expressed using non-linear Chi–square test ($\chi 2$) must be relatively low.

3 Results and discussion

3.1 Moisture content and UV–visible spectroscopy

The moisture content of *Vigna unguiculata* stem was determined by oven drying and was found to be 25.89 ± 0.51%. The synthesis of AgNPs was visually confirmed by a change in colour of the silver nitrate solution into a dark brown-coloured solution. The colour change is due to vibration of the metal nanoparticles in the electronic energy levels, leading to the emergence of SPR bands characteristic to the metal. A characteristic wavelength band at 450–460 nm (455 nm) further confirmed the formation of AgNPs (Fig. 1). The absorbance increased with time, connoting the formation of larger particles, in consonance with Smith et al. [18] who suggested that the longer the reaction time, the larger the nanoparticle size.

The close proximity of the conduction band and valence band in silver nanoparticles, like most noble metal nanoparticles, allows easy oscillation of free electrons between the bands giving rise to a surface plasmon resonance (SPR) absorption band. The phenomenon, Surface Plasmon Resonance, occurs as a result of collective oscillation of free electrons of the nanoparticles in resonance with the frequency of the incident light wave, usually in the visible or UV region, interacting with the nanoparticles. Fundamentally, SPR absorption peaks are exclusive to metal nanoparticle only thereby making the existence of SPR peak a fingerprint of metal nanoparticle formation. Shift in SPR bands towards the red end or blue end depends on particle size, shape, state of aggregation and the surrounding dielectric medium [19].

3.2 Fourier transform infra-red (FTIR) analysis of the AgNPs

The spectrum showing the functional groups present in the synthesized AgNPs from *Vigna unguiculata L.* stem is as shown in Fig. 2. The possible biomolecules in the AgNPs showed characteristic absorption bands at wave numbers (cm^{-1}) 3413.46, 2927.64, 1592.17, 1388.48, 1023.64, 612.5, 539.54. The absorption peaks were assigned N–H stretching in alkaloids; C–H stretching vibrations; –C=C– in the aromatic rings of the biomolecules or possible –N–H bend; –C–N– stretching vibrations of amine, –C–O– stretching vibrations and bands 612.5, 539.54 cm^{-1} due to –C–Br– or –C=C– benzene vibrations. The observed peaks suggested the capping of the nanoparticles by alkaloids present in *Vigna unguiculata L.* stem.

In addition, Fig. 2 showed the superimposed FTIR spectrum of the AgNPs before and after adsorption. The spectra indicated the bands remained essentially

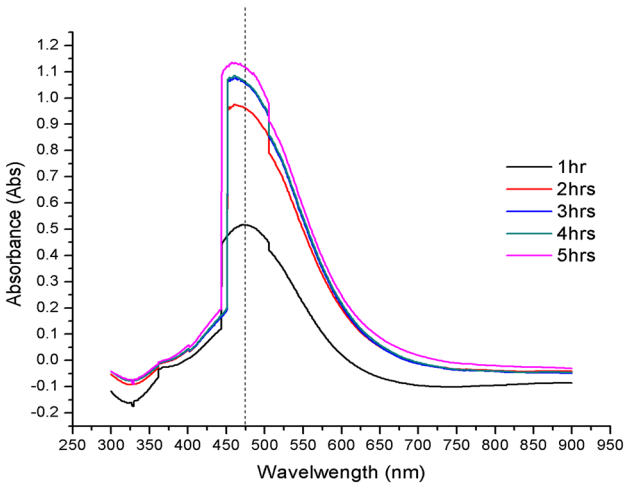

Fig. 1 UV–Vis Spectra of AgNPs

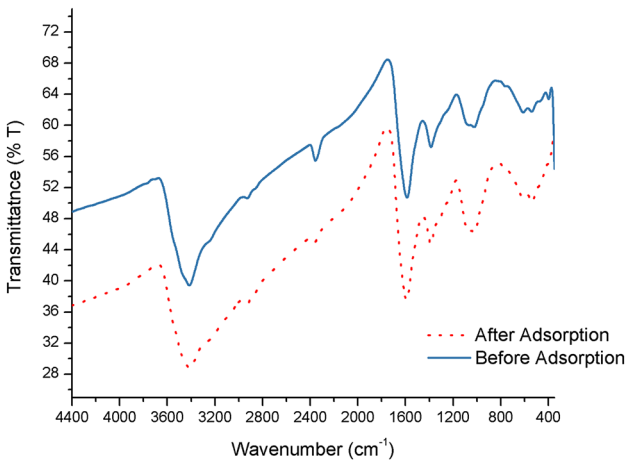

Fig. 2 FT-IR spectrum of AgNPs before and after adsorption

unchanged even after the adsorption. Therefore, the FTIR spectra suggested that electrostatic interactions between the adsorbate molecules and AgNPs adsorbent surface is predominantly responsible for the adsorption of MG dye.

3.3 Scanning electron microscopy (sem)-energy dispersive x-ray (EDX)

The surface morphology and elemental composition of AgNPs was obtained by SEM and EDX analysis. Figure 3 showed the SEM image of the synthesized AgNPs.

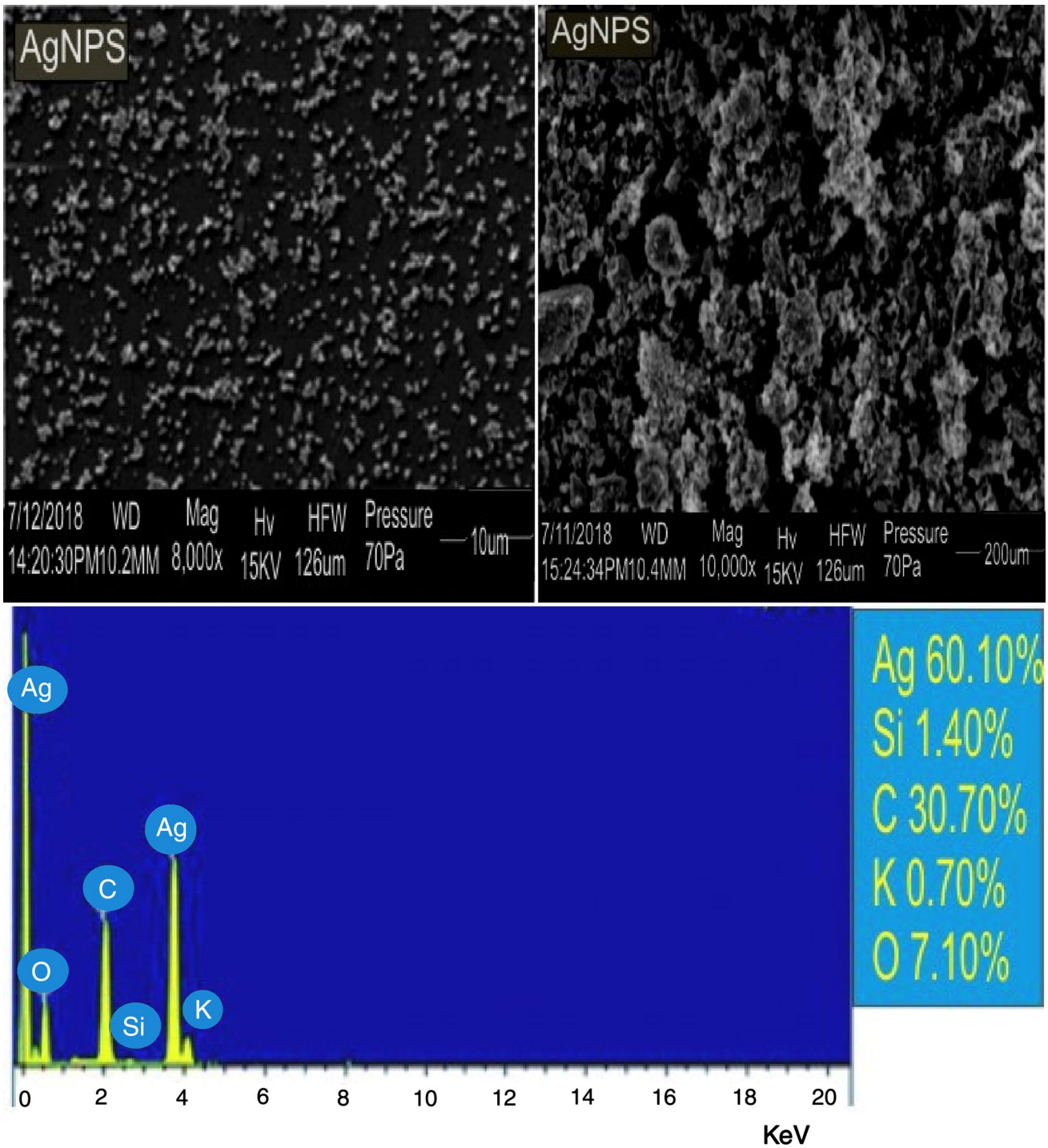

Fig. 3 The SEM-EDX micrograph of synthesized AgNPs

The resolution limit of the SEM prohibits distinguishing individual AgNPs, thus the size of the nanoparticles that assembled into spheres could not be estimated accurately. EDX analysis provides the elemental composition of sample. Figure 3 also showed the elemental composition of unloaded AgNPs. The results revealed sharp peaks of the elements Ag, C and smaller peaks of the elements such as, Si, K, and O. The elemental analysis (%) showed: Ag, 60.10; Si, 1.40; C, 30.70; K, 0.70 and O, 7.10.

3.4 X-ray diffraction (XRD)

The AgNPs synthesized from *Vigna unguiculata* L. stem extract were confirmed by the characteristic peaks observed in the XRD micrograph (Fig. 4). The diffracted intensities were recorded from 20° to 80°. Four strong Bragg reflections corresponds to the planes of (100), (101), (110), and (222) that can be indexed according to the facets of face centered cubic crystal structure of silver. The inter-planar spacing ($d_{calculated}$) values are 2.336, 1.955, 1.436 and 1.224 Å for (100), (101), (110) and (222) planes respectively and matched with standard silver values. The Debye–Scherrer formula was used to calculate the average crystalline size,

$$D = \frac{k\lambda}{\beta \cos\theta} \quad (5)$$

where D is the average crystalline size of the nano-particles, k is geometric factor (0.9), λ is the wavelength of X-ray radiation source and β is the angular FWHM (full-width at half maximum) of the XRD peak at the diffraction angle θ. The calculated average crystalline size of the AgNPs is ~ 25 nm.

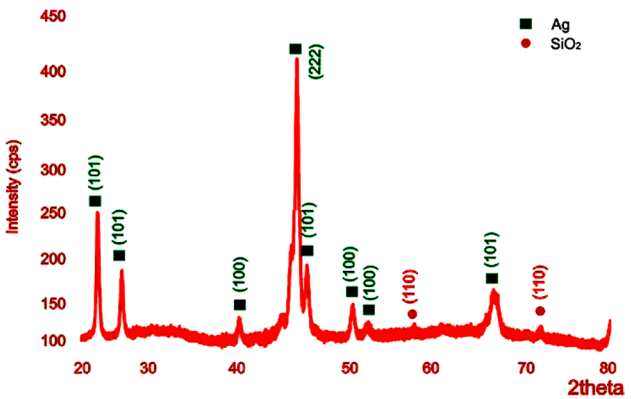

Fig. 4 XRD micrograph of synthesized AgNPs

3.5 Effect of pH_{pzc} of adsorbent and pH of adsorbate

The pH of the adsorbate solution plays a pivotal role in adsorption as it influences the surface charge of the adsorbent and mobility of the adsorbate [20]. The effect of pH of adsorbate (MG) on its adsorption using AgNPs is represented in Fig. 5. The pH_{pzc} for AgNPs was found to be 8.6 from the point of intersection with the pH_i axes as represented in Fig. 6. The point of zero charge (pH_{pzc}) is the pH where the net charge on the adsorbent surface, in this case AgNPs, is zero. From experimental data, it was found that the adsorption capacity, qe (mg/g) increased from 17.65 to 80.39 at pH 3 to 9 after which it remained constant and then dropped at pH 12.

Based on the concept of pH_{pzc}, at pH above the pH_{pzc}, the surface of the adsorbent will be predominantly negatively charged while net positive charge would be obtained when solution pH is below the pH_{pzc}. At pH less than 8.6, the adsorbent surface was highly cationic and electrostatic repulsion is experienced between the

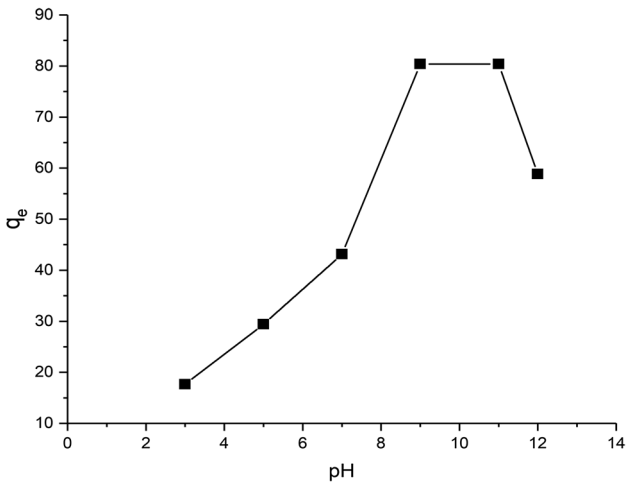

Fig. 5 Effect of pH on the adsorption of MB by AgNPs

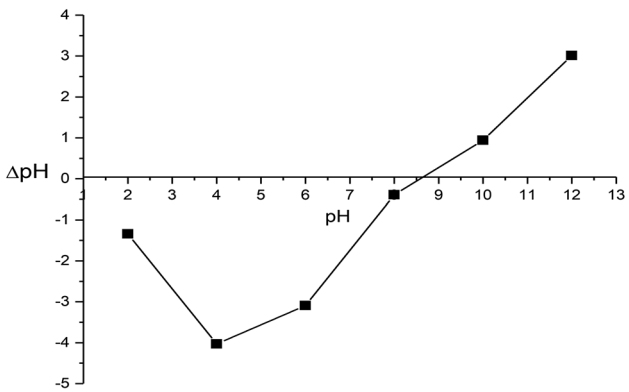

Fig. 6 Determination of pH of point of zero charge of AgNPs

adsorbent and adsorbate resulting a low adsorption capacity. At pH 9, AgNPs surface becomes anionic which favors the adsorption of cationic dyes due to increase in electrostatic force of attraction.

3.6 Effect of contact time

The effect of contact time is one of the most important factors in batch adsorption process as it ensures that the equilibrium of the adsorbent–dye system is attained. The effect of contact time is summarized in Fig. 7. The percentage removal and adsorption capacity (q_e) at a time (t) increased rapidly with an increase in contact time initially, and thereafter a contact time of 40 min beyond which no noticeable change was observed. The rapid dye adsorption at the initial stage is believed to be as a result of the availability of vacant sites on the adsorbent surface at the beginning of the adsorption process which gradually became scarce over time until the point where all possible adsorption sites were occupied. At which point, equilibrium is reached between the adsorbent and the dye. This is in agreement with the trend reported by Azeez et al. [20].

3.7 Effect of temperature

The temperature dependency of the adsorption of MG dye on AgNPs is represented in Fig. 8. The adsorption capacity decreased from 37.25 to 7.84 mg/g as the temperature increased from 30 to 50 °C. This phenomenon suggests that the adsorption process is an exothermic one and that low temperature is the most favourable condition for adsorption of MG dye using AgNPs. This observation may be as a result of increased entropy and mobility of the molecules of the dye with increase in temperature.

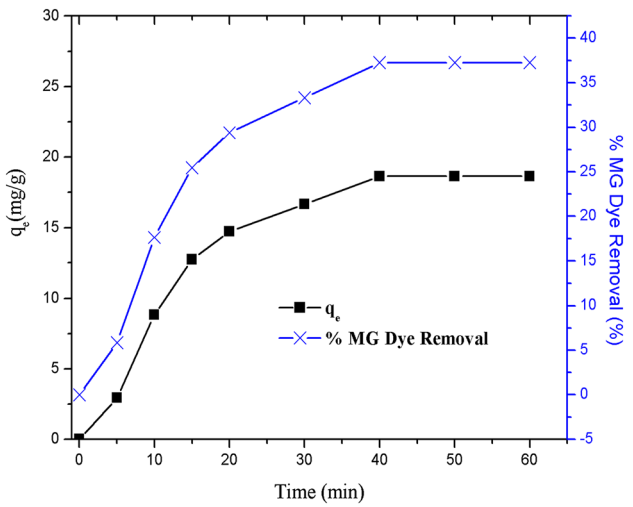

Fig. 7 Effect of contact time on the removal of MG by AgNPs

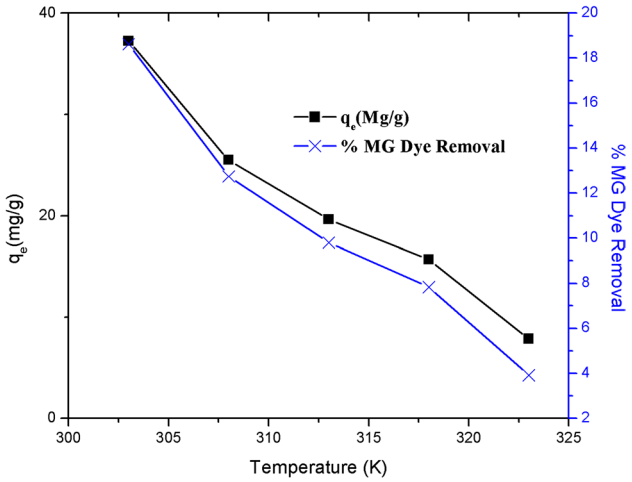

Fig. 8 Effect of temperature on the removal of MG by AgNPs

3.8 Effect of initial dye concentration

The impact of initial dye concentration is the basis for all adsorption isotherm models. Figure 9 showed an upward trend of the MG dye adsorption (q_e) with increase in concentration. At higher dye concentration, the dye molecules were adsorbed more than lower concentrations as more dye molecules were available for interaction with the adsorbent sites. The percentage of MG removed however decreased after 200 mg/L and the concentration of 200 mg/L was used for other batch experimental studies.

3.9 Effect of adsorbent concentration

Concentration of the adsorbent determines the adsorption capacity of an adsorbent for a given initial concentration of

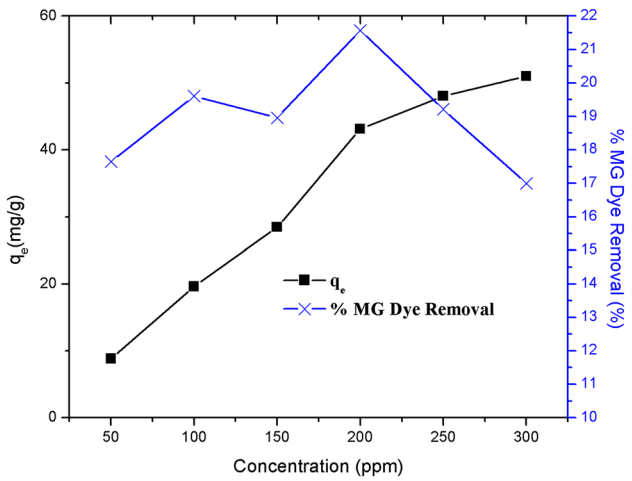

Fig. 9 Effect of initial dye concentration on the removal of MG by AgNPs

the adsorbate at given operating conditions. The effect of adsorbent concentration on adsorption of MG was studied in range 0.4–2.0 g. Figure 10 showed that the percentage MG removal increased from 15.69 to 50% as the concentration of adsorbent increased from 0.4–2.0 g. The observed trend is attributed to an increase in adsorbent surface and the number of sites available for adsorption [17].

3.10 Adsorption isotherm evaluation for MG dye removal using AgNPs

For accurate examination of the relationship between the amount of MG dye adsorbed and its concentration, Langmuir, Temkin, Freundlich and Dubinin–Radushkevich isotherm models were employed. The parameters obtained from the plots are represented in Table 1. Correlation coefficient (R^2) and the residual sum of squares (RSS) were used to determine which model best describes the adsorption process. The closer the R^2 to unity and the lower the RSS values, the better the agreement between experimental data, and model. At which point we can describe the isotherm as being the best fit to describe the adsorption process. Comparing R^2 and RSS for each isotherm, the Langmuir isotherm best fits the adsorption of MG dye using AgNPs. This implies the adsorption process is a monolayer and homogenous adsorption with finite number of available adsorption sites possessing equal affinity for adsorbate molecules and also with neighboring adsorbate molecules in no way interacting with each other. The value of R_L, which is an indicator of the favorability of the adsorption process, was calculated for Langmuir adsorption constant (K_L). As shown in Table 1, R_L is 0.809192 ($0 < 0.809192 < 1$), confirming that the adsorption process was favorable.

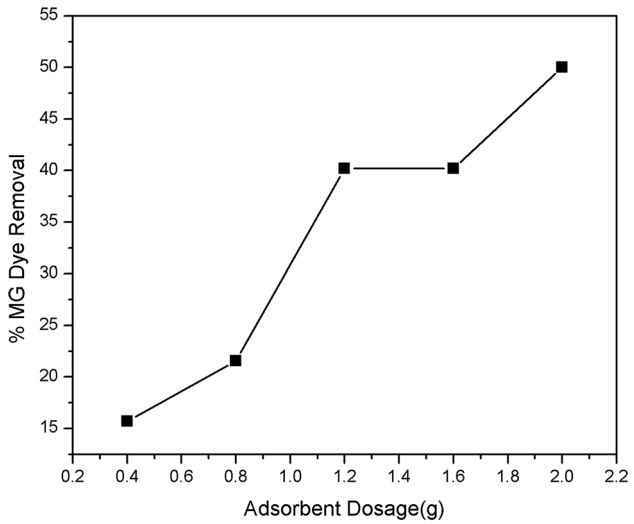

Fig. 10 Effect of adsorbent dose on the removal of MG by AgNPs

3.11 Adsorption kinetics

The controlling mechanism and rate of the adsorption of MG dye unto AgNPs were studied in order to understand the adsorption kinetics. The parameters obtained for Pseudo-first-order, Pseudo-second order, Elovich kinetic models, and intra-particle diffusion model are shown in Table 2. Correlation coefficient (R^2) and non-linear Chi–square test ($\chi 2$) were used to explore the similarity between experimental and calculated data. The model that best describes the adsorption process must have R^2 values closest to unity and a relatively low ($\chi 2$) value. Comparison of correlation coefficients of pseudo-first order, pseudo-second order and Elovich kinetic models (Table 2) show that pseudo-first order best describes the mechanism and rate of adsorption of MG on AgNPs. Equally important, the lower value of $\chi 2$ further confirms pseudo-first order as the best fit kinetic model. This suggests that the adsorption of MG dye on AgNPs may be inclined towards physisorption [17].

Intra-particle diffusion, among other factors, controls the rate of adsorption. The possibility of intra-particle diffusion having an influence on the adsorption process was studied (Table 2). The rate controlling step in the adsorption process was further investigated using the Elovich model (Table 2). The linear plot for intra-particle

Table 1 Adsorption isotherms parameters for the removal process onto AgNPs

Isotherms	Equation	R^2	RSS	Constants	Values
Langmuir	$\frac{1}{q_e} = \frac{1}{q_{max}} + \frac{1}{C_e q_{max} K_L}$	0.99194	5.23541×10^{-5}	q_{max} (mg/g)	268.82
				K_L	7.86×10^{-4}
				R_L	0.81
Temkin	$q_e = B \ln A + B \ln C_e$	0.95974	57.84293	B	25.15
				A	0.03
Freundlich	$\log q_e = \frac{1}{n} \log C_e + \log K_f$	0.97684	0.01003	n	0.9869
				K_f	0.22
D-R	$\ln q_e = \ln q_0 - \beta\varepsilon^2$	0.85524	0.26602	β	480.14
				Q_0	43.61

Table 2 Adsorption kinetics parameters for the removal process onto AgNPs

Kinetics	Equation	R^2	χ^2	Constants	Values
Pseudo-first order	$\log(q_e - q_t) = \log q_e - \frac{K_1}{2.303}t$	0.98976	0.183773	$K_1(min^{-1})$	0.079223
				$q_{e(calc)}$ (mg/g)	20.48
Pseudo-second order	$\frac{t}{q_t} = \frac{1}{K_2(q_e)^2} + \frac{1}{q_e}t$	0.95548	25.154659	K_2 (g/mg min)	3.5×10^{-4}
				$q_{e(calc)}$(mg/g)	40.27
Elovich	$q_t = \frac{1}{\beta}\ln\beta\alpha + \frac{1}{\beta}\ln t$	0.98698		B	0.13
				A	2.41
Intra-particle diffusion	$q_t = K_{diff}t^{1/2} + C$	0.92937		K_{dif} (mg/g $min^{-1/2}$)	3.69
				C (intercept)	3.29

diffusion model has a correlation coefficient R^2 of 0.92937 which indicates the involvement of intra-particle diffusion in the adsorption process. However, the linear plot did not pass through the origin, suggesting that intra-particle diffusion was not the sole rate-determining step. The Elovich plot also did not pass through the origin, thus corroborating the suggestion. Therefore, surface adsorption and intra-particle diffusion occurred concurrently during adsorption process. From intraparticle diffusion, the larger the intercept value of *C*, the greater the boundary layer diffusion effect [20–22].

4 Conclusion

This report shows a novel route for the synthesis of AgNPs using stem extract of readily available, *Vigna unguiculata L* and its application as adsorbent for malachite green (MG). The synthesized AgNPs was characterized using UV–Vis Spectroscopy, FTIR, SEM and XRD. The Initial pH, contact time, initial dye concentration, adsorbent concentration and temperature affected the adsorption process. Batch adsorption of MG dye was also carried out on the synthesized AgNPs. Adsorption isotherm and kinetic models were used to describe the adsorption process. Langmuir isotherm was the best fit for the experimental data with maximum monolayer adsorption capacity of 268.82 mg/g. The adsorption followed Pseudo-first-order kinetics and was controlled by intra-particle diffusion and surface adsorption. The synthesized AgNPs can be used as adsorbent for MG, however, the relatively low percentage removal (21.6% at 200 mg/L) of MG dye suggest that silver nanoparticle, synthesized from *Vigna unguiculata L*. stem, alone may not be sufficient in the complete adsorption of MG dye.

Compliance with ethical standards

Conflict of interest The authors declare no conflict of interest in this research work.

References

1. Ali I, Gupta VK (2007) Advances in water treatment by adsorption technology. Nat Protoc 1:2661–2669
2. Caponi N, Collazzo CG, Jahn SL, Foletto LE (2016) Use of Brazillian Kaolin as a potential low cost adsorbent for the removal of malachite green colored effluent. Mater Res 10(3):5–7
3. Song Y, Ding S, Chen S, Xu H, Mei Y, Ren J (2015) Removal of malachite green in aqueous solution by adsorption on sawdust. Korean J Chem Eng 32:2443–2448
4. Worch E (2012) Adsorption technology in water treatment: fundamentals, processes, and modeling. De Gruyter, Boston, Berlin
5. Agbogidi OM, Egho EO (2012) Evaluation of eight varieties of cowpea (*Vigna unguiculata*(L.) Walp) in Asaba agro-ecological environment, Delta State, Nigeria. Eur J Sustain Dev 1(2):303–314
6. Brissibe EA, Adugbo SE, Ekanem UF, Figuerira GM (2011) Controlling Bruchid Pest's pest of stored cowpea seeds with dried leaves of *Artemesia annua* and two other botanicals. Africa J Biotechnol 10(47):9586–9592
7. Ndong A, Kebe KH, Thiaw CH, Diome T, Senbene M (2012) Genetic distribution of the cowpea (*Vigna unguiculata L.*) Walp (*Bruchid callosobruchus malculatus F. Coleoptera, bruchidae*) population in different agro-ecological area of West Africa. J Animal Sci Adv 2(7):616–630
8. Islam MS, Choi WS, Nam B, Yoon C, Lee HJ (2017) Needle like iron oxide@$CaCO_3$ adsorbents for ultrafast removal of anionic and cationic heavy metal ions. Chem Eng J 308:208–219
9. Aziagba BO, Okeke CU, Ezeabara AC, Ilodibia CV, Ufele AN, Egboka TP (2017) Determination of the flavonoid composition of seven varieties of *Vigna unguiculata*(L.) Walp as food and therapeutic values. Uni J Appl Sci 5(1):1–4
10. Tony N, James O, Nixon T (2014) Cowpea production handbook. College of Natural Resources and Environmental Studies, University of Juba, Juba
11. Khataee AR, Dehghan G, Ebadi A, Zarei M, Pourhassan M (2010) Biological treatment of a dye solution by *Macroalgae-Chara Sp.*: effect of operational parameters, intermediates

identification and artificial neural network modelling. Biores Technol 101:2252–2258
12. Muthu AK, Karthikeyan C, Rajasimman M (2017) Isotherm and kinetic studies on adsorption of malachite green using chemically synthesized silver nanoparticles. Nanotechnol Environ Eng 2:2–7
13. Charumathi D, Femila EM, Srimathi R (2014) Removal of malachite green using silver nanoparticles via adsorption and catalytic degradation. Inter J Pharm Pharm Sci 6(8):579–583
14. Pandian AMK, Karthikeyan C, Rajasimman M (2017) Isotherm and kinetic studies on adsoption of malachite green using chemically synthesized silver nanoparticles. Nanotechnol Environ Eng 2:2. https://doi.org/10.1007/s41204-016-0013-4
15. Vanaja M, Paul-Kumar K, Baburaja M, Rajeshkumar S, Ganana-Jobitha G, Malarkodi C (2014) Degradation of methylene blue using biologically synthesized silver nanoparticles. J Bioinorg Chem Appl 1:1–7
16. Pandian AMK, Karthikeyan C, Rajasimman M (2016) Isotherm and kinetic studies on nano-sorption of malachite green onto *Allium sativum* mediated synthesis of silver nano particle. Biocatal Agric Biotechnol 8:171–181
17. Dawodu FA, Akpomie KG (2014) Simultaneous adsorption of Ni(II) and Mn(II) ions from aqueous solution unto a Nigerian kaolinite clay. J Mater Res Technol 3:128–141
18. Smith AM, Duan H, Rhyner MN, Ruan G, Nie S (2006) A systematic examination of surface coatings on the optical and chemical properties of semiconductor quantum dots. Phys Chem Chem Phys 8(33):3895–3903
19. Lufsyi M, Edi S, Agung B, Setio U, Kamsul A (2015) Optical properties of silver nanoparticles for surface plasmon resonance (SPR)-based biosensor applications. J Mod Phys 6:1071–1076
20. Azeez LA, Segun AA, Abdulrasaq OO (2018) Novel biosynthesized silver nanoparticles from cobweb as adsorbent for *Rhodamine B*: equilibrium isotherm, kinetic and thermodynamic studies. Appl Water Sci 8:32–43
21. Weber WJ, Morris JC (1963) Kinetics of adsorption on carbon from solution. J San Eng Div Am Soc Civil Eng 89:31–60
22. Eze SI, Akpomie KG, Ezeofor CC, Osunkunle AA, Maduekwe OB, Okenyeka OU (2019) Isotherm and kinetic evaluation of *Dialium guineense* seed husk and its modified derivatives as efficient sorbent for crude oil polluted water treatment. Water Conserv Sci Eng. https://doi.org/10.1007/s41101-019-00065-6